

Supplement of Atmos. Chem. Phys., 17, 10435–10465, 2017
<https://doi.org/10.5194/acp-17-10435-2017-supplement>
© Author(s) 2017. This work is distributed under
the Creative Commons Attribution 3.0 License.



Supplement of

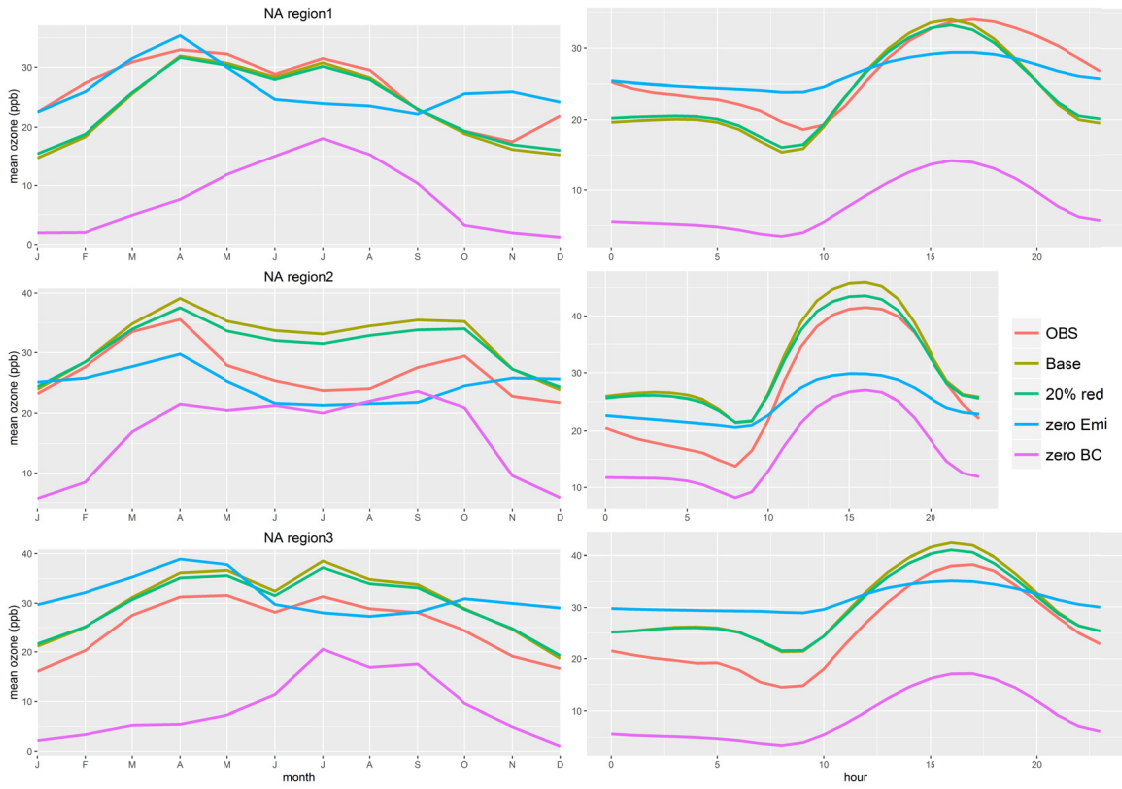
Advanced error diagnostics of the CMAQ and Chimere modelling systems within the AQMEII3 model evaluation framework

Efisio Solazzo et al.

Correspondence to: Efisio Solazzo (efisio.solazzo@ec.europa.eu)

The copyright of individual parts of the supplement might differ from the CC BY 3.0 License.

4 SUPPLEMENTARY FIGURES

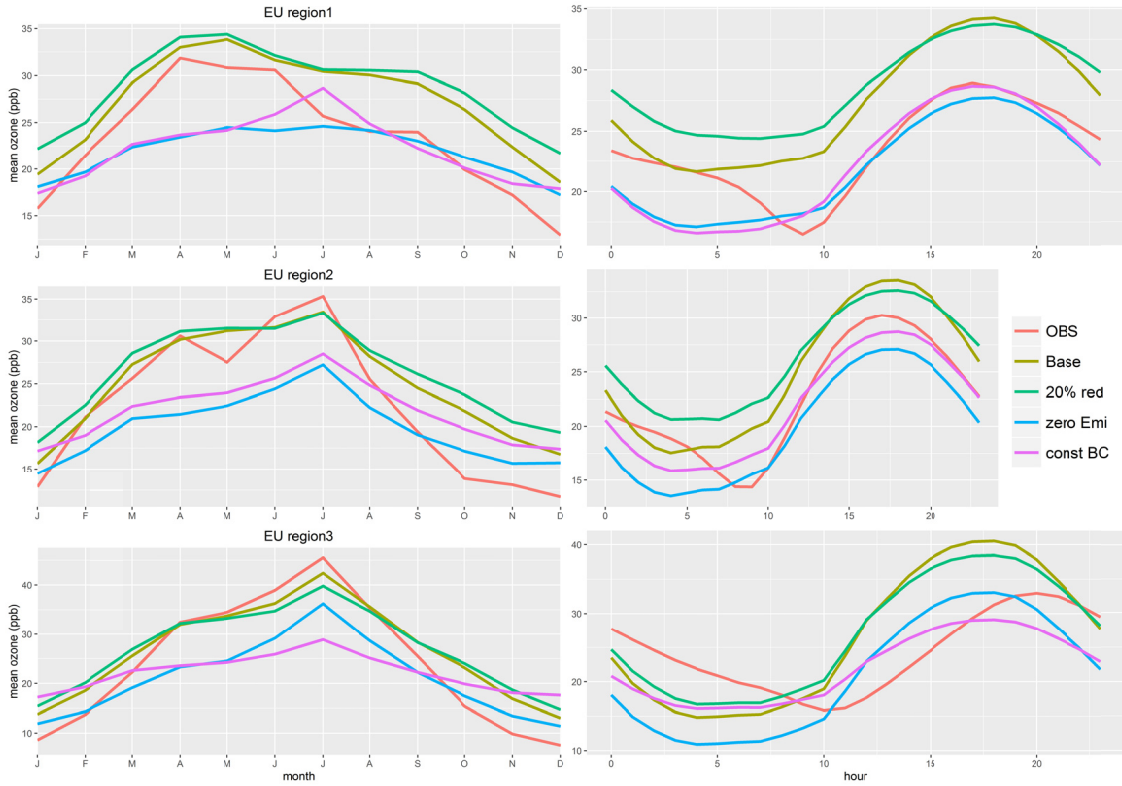


5

9 **FIGURE S1** Annual aggregated ozone time series for the North American sub-regions (Urban stations only).
 10 Average monthly and diurnal curves

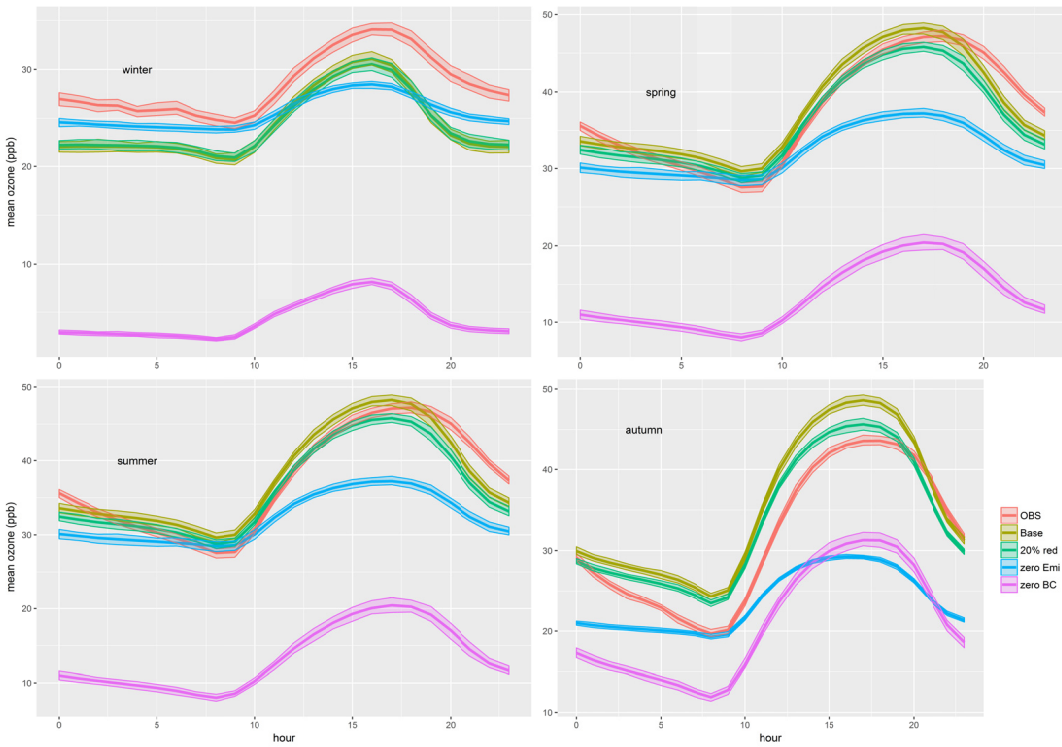
8

9



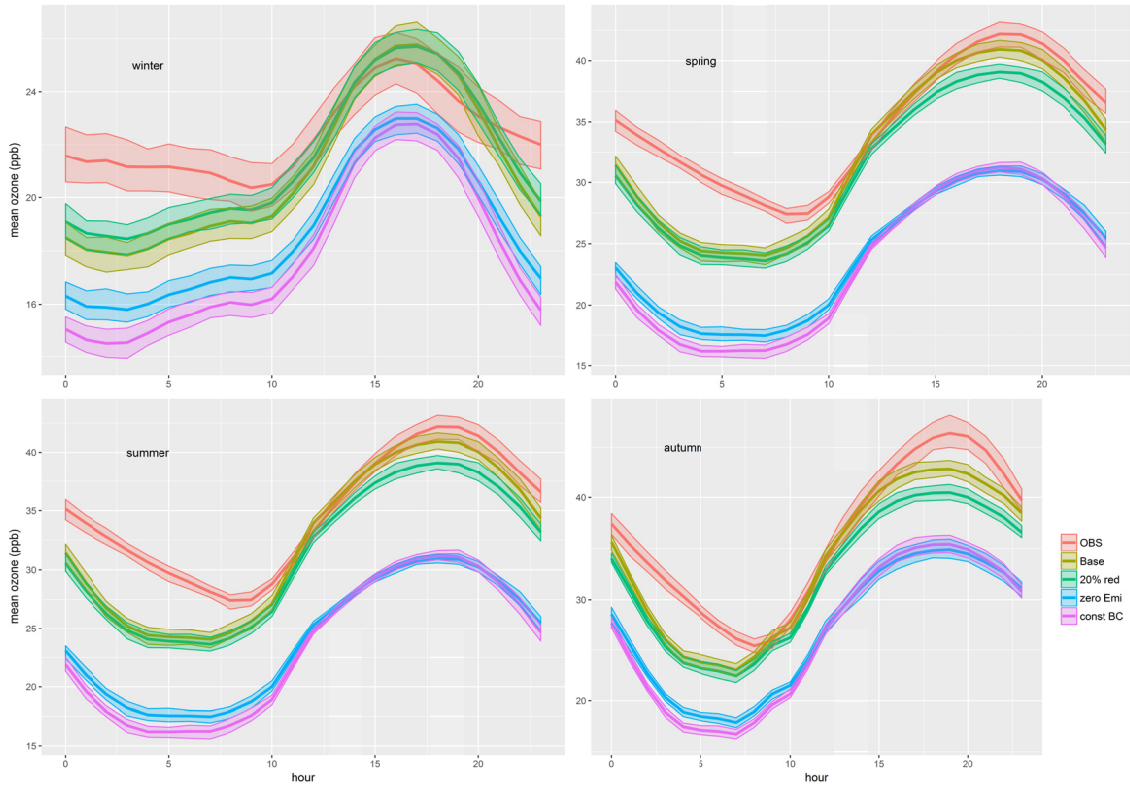
10

14 **FIGURE S2.** Annual aggregated ozone time series for the European sub-regions (urban stations only). Average
 15 monthly and diurnal curves



13

17 **FIGURE S3** Network average seasonal daily ozone profiles for North America. The confidence bands indicate the 95% confidence interval of
 18 the mean



16

20 **FIGURE S4.** Network average seasonal daily ozone profiles for Europe. The confidence bands indicate the 95%
 21 confidence interval of the mean

19

20

21

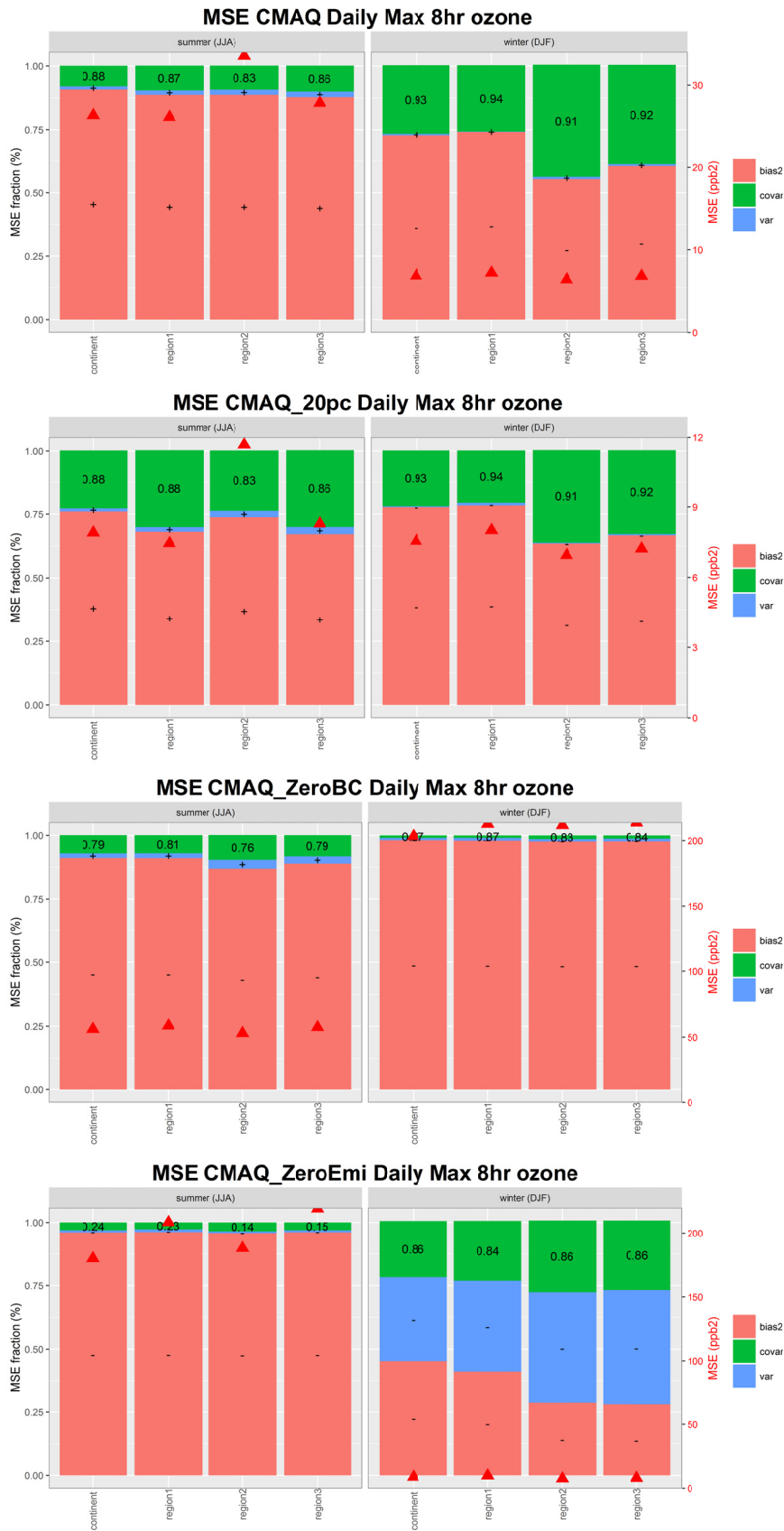
22

23

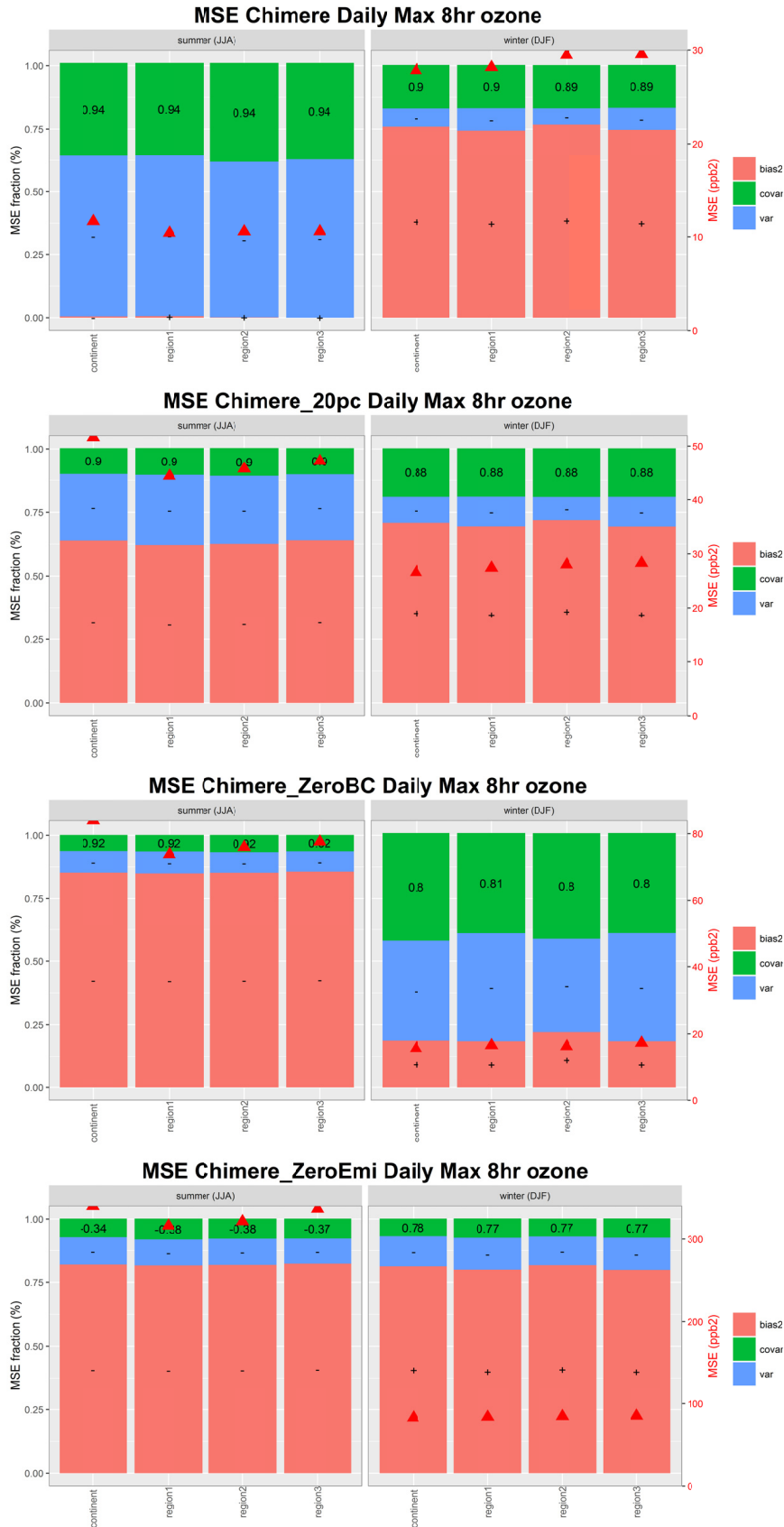
24

25

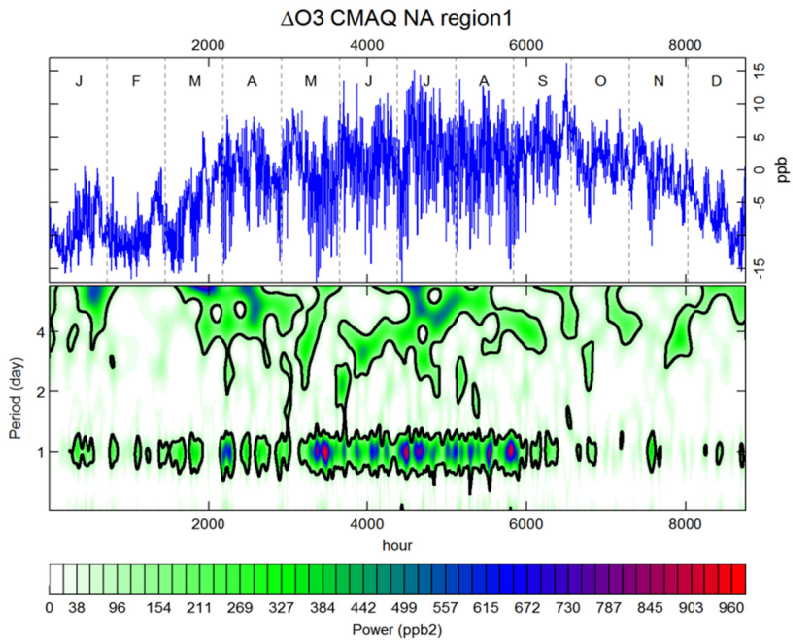
26



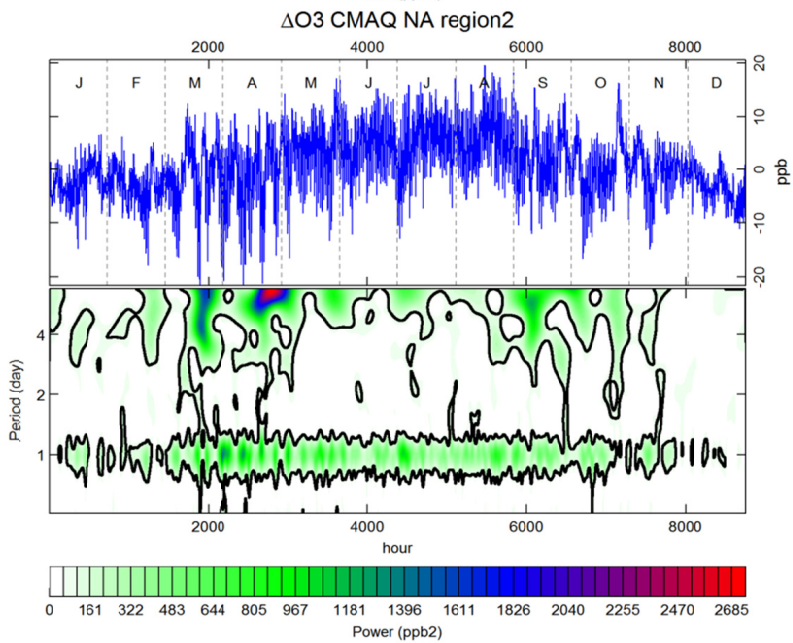
27 FIGURE S5. Same as Figure 6 to Figure 10 of the main text for the daily maximum 8-hour rolling average ozone



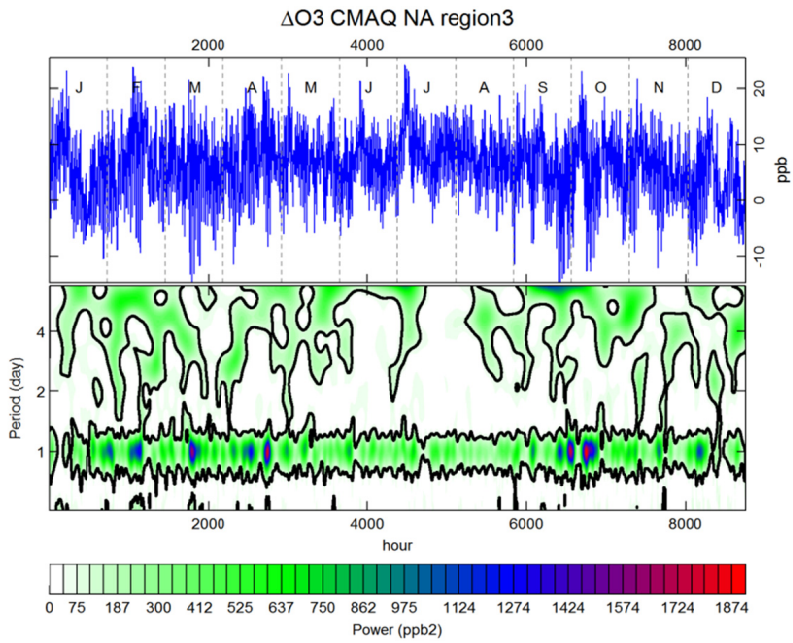
28 FIGURE S6. Same as Figure 11 to Figure 15 of the main text for the daily maximum 8-hour rolling average ozone



32



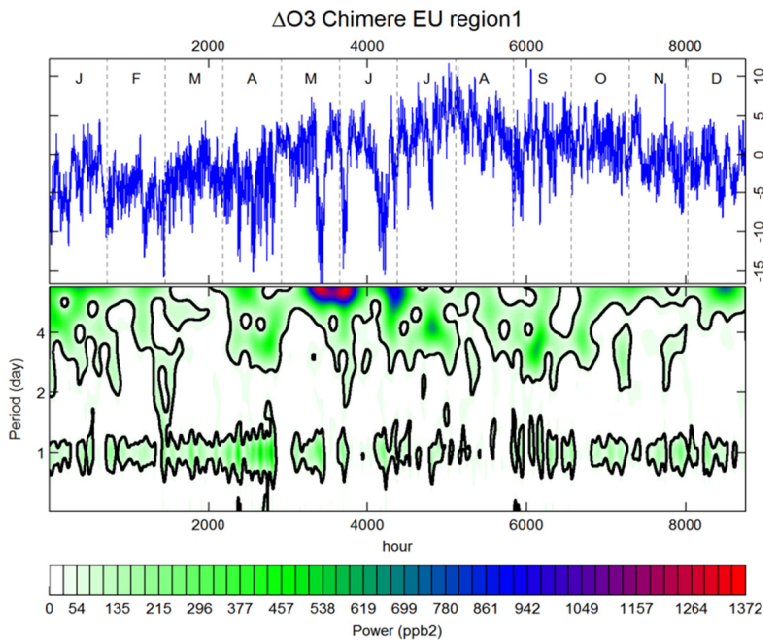
33



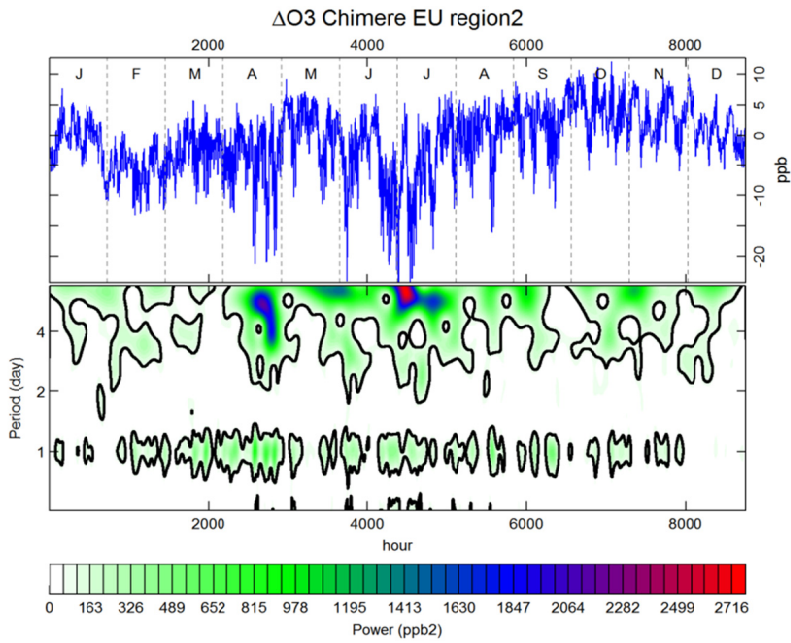
31

41 **FIGURE S7.** Annual time series of differences between CMAQ and observed O_3 (ΔO_3 , top panel) and Morlet
 42 wavelet analysis of the periodogram of ΔO_3 (lower panel) for the three NA subdomains, for periods between
 43 0.5 and 6 days. Black contours lines identify the 95% confidence interval. The period (in days) is reported in the
 44 vertical axis, while the quantiles of the power spectral density are measured in ppb^2 .

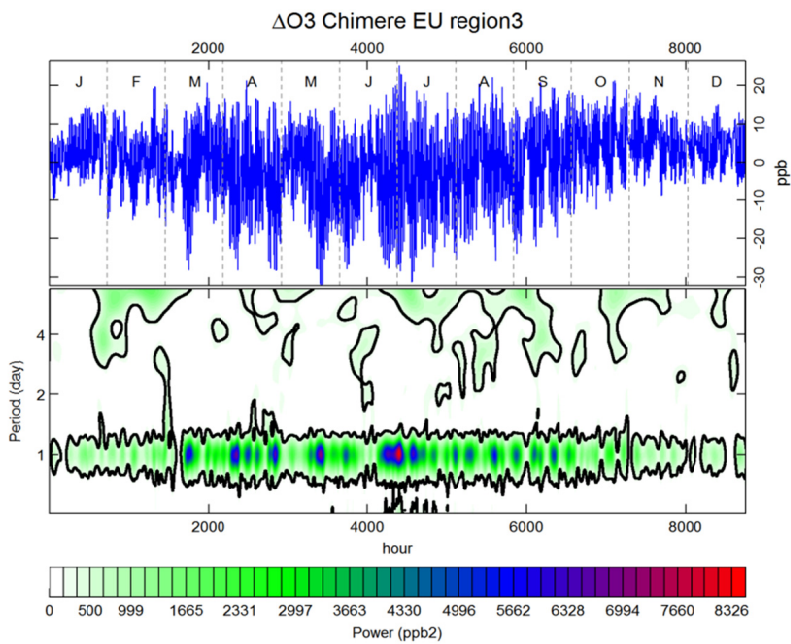
36



37



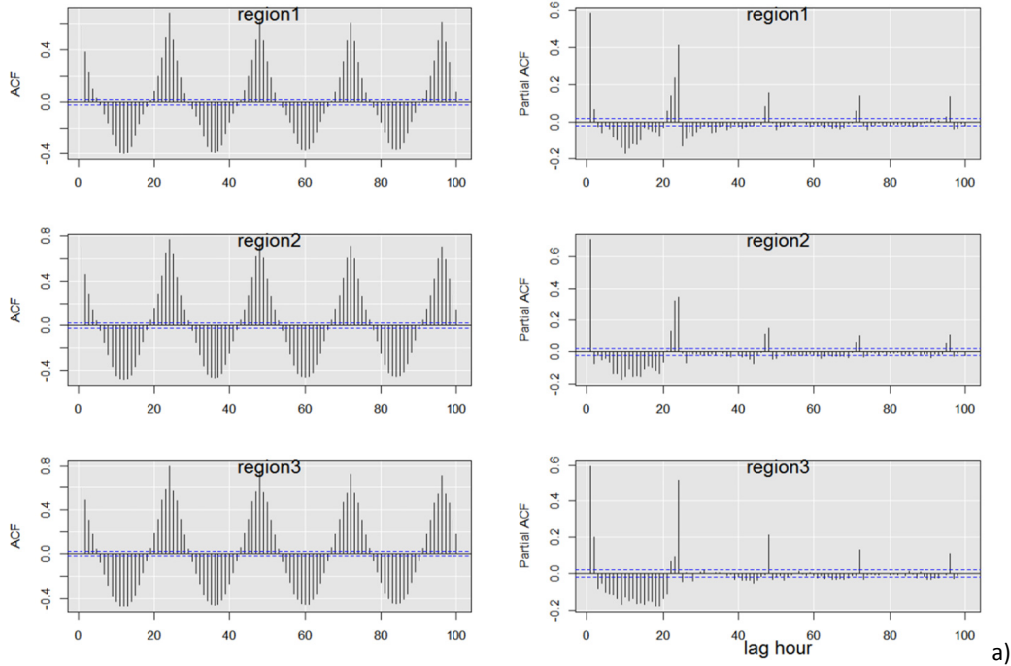
38



39

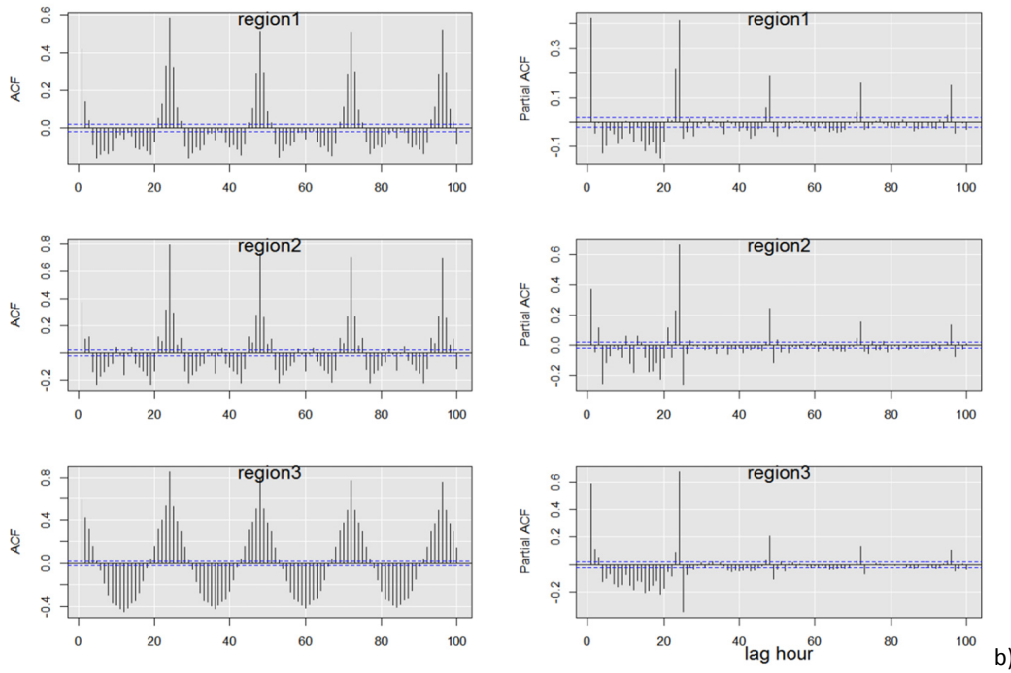
49 **FIGURE S8.** Annual time series of differences between Chimere and observed O_3 (ΔO_3 , top panel) and Morlet
 50 wavelet analysis of the periodogram of ΔO_3 (lower panel) for the three EU subdomains, for periods between
 51 0.5 and 6 days. Black contours lines identify the 95% confidence interval. The period (in days) is reported in the
 52 vertical axis, while the quantiles of the power spectral density are measured in ppb^2 .

CMAQ ACF and PACF for ΔO_3 zero EMI



44

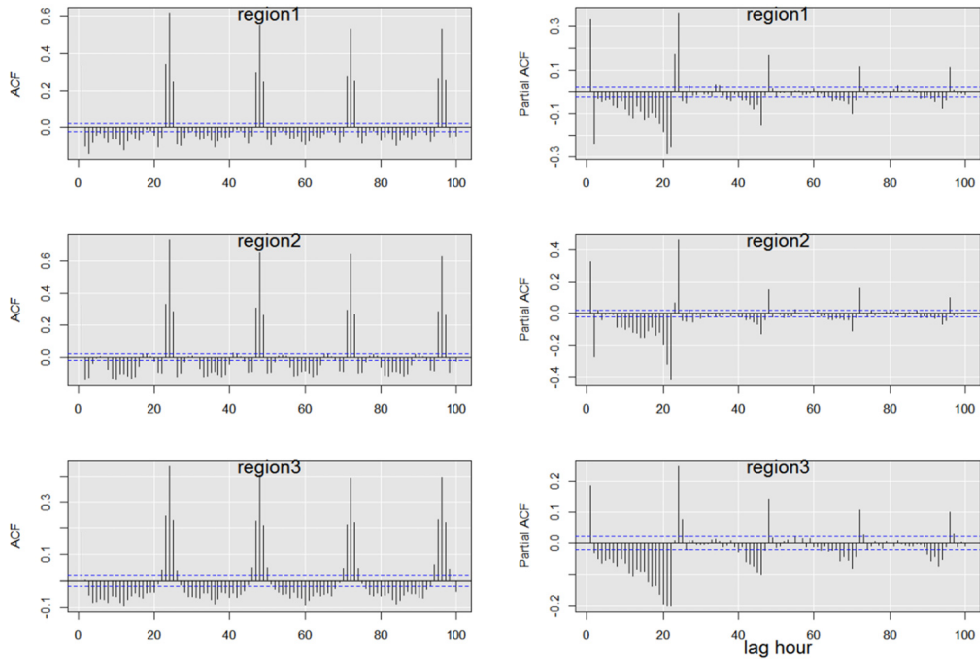
Chimere ACF and PACF for ΔO_3 zero EMI



45

49 **FIGURE S9.** Autocorrelation (ACF) and partial autocorrelation (PACF) function for the differenced time series of
 50 residuals of ozone (mod-obs) for the 'zero EMI' scenario for a): CMAQ and b): Chimere.

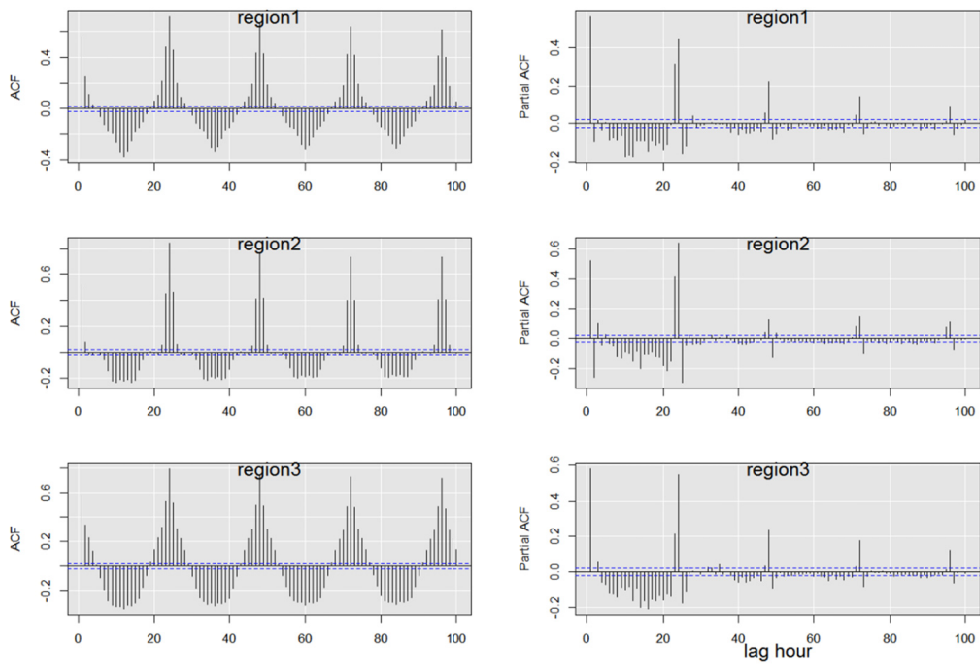
CMAQ ACF and PACF for Δ WS



51

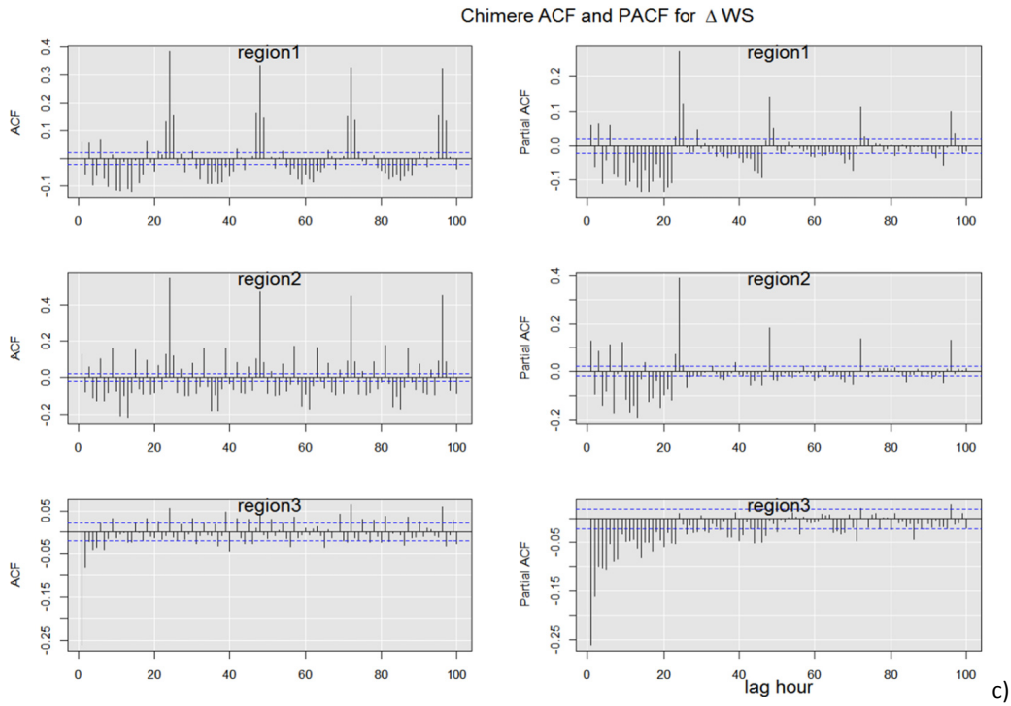
a)

CMAQ ACF and PACF for Δ Temp

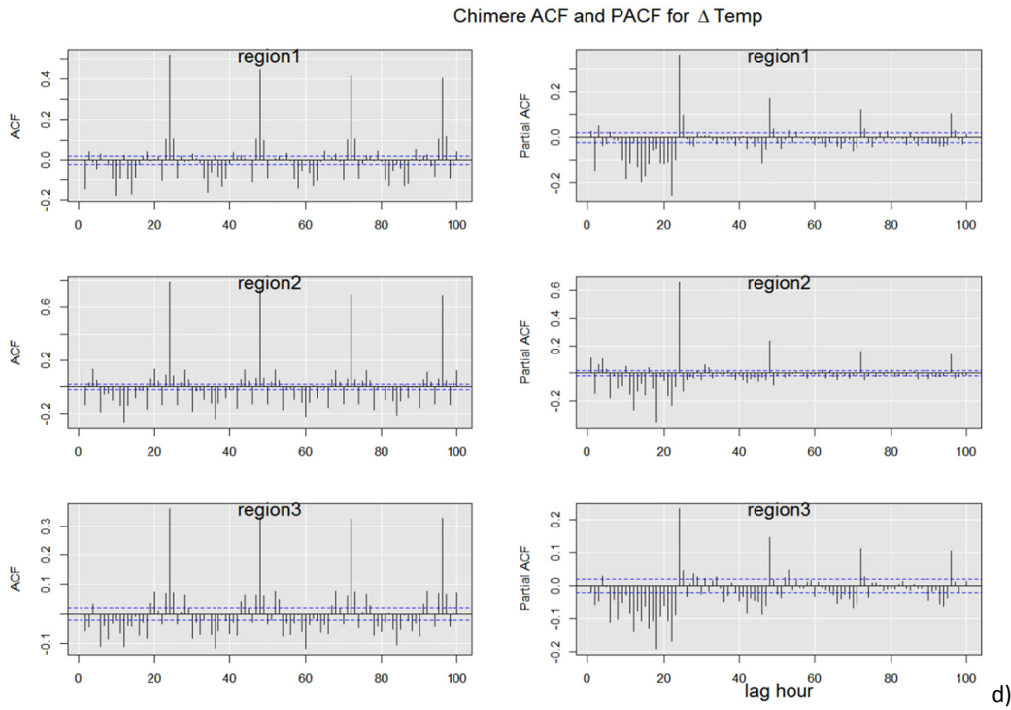


52

b)



50

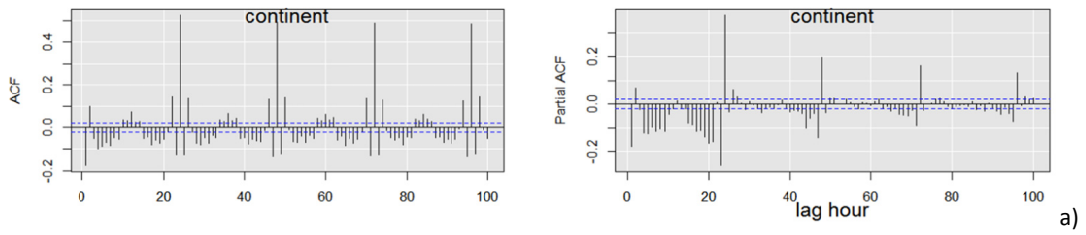


51

55 **FIGURE S10.** Autocorrelation (ACF) and partial autocorrelation (PACF) function for *a)* the differenced time series
 56 of residuals of WS (mod-obs) (*a)*: CMAQ, *c)*: Chimere) and Temp (*b)*: CMAQ, *d)*: Chimere).

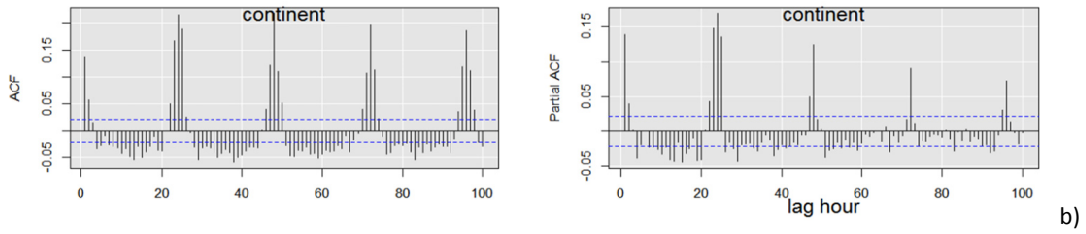
54

CMAQ ACF and PACF for Δ CO



55

Chimere ACF and PACF for Δ PM10



56

60 **FIGURE S11** Autocorrelation (ACF) and partial autocorrelation (PACF) function for the differenced time series of
61 residuals (mod-obs) of a) CO in NA and b) PM₁₀ in EU.

59

60

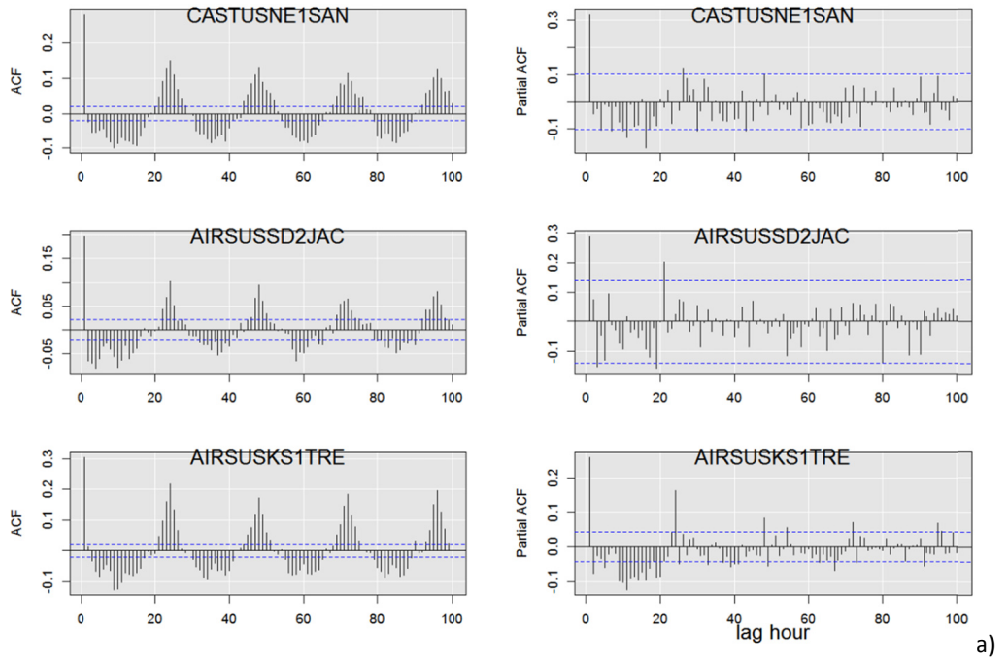
61

62

63

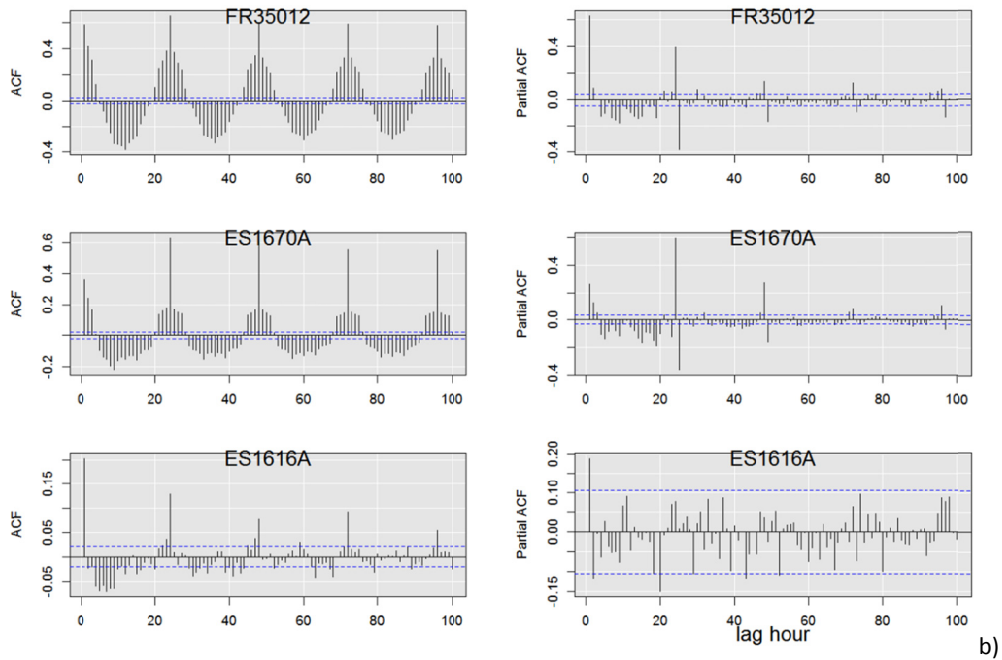
64

CMAQ ACF and PACF for ΔO_3 stations



65

Chimere ACF and PACF for ΔO_3 stations

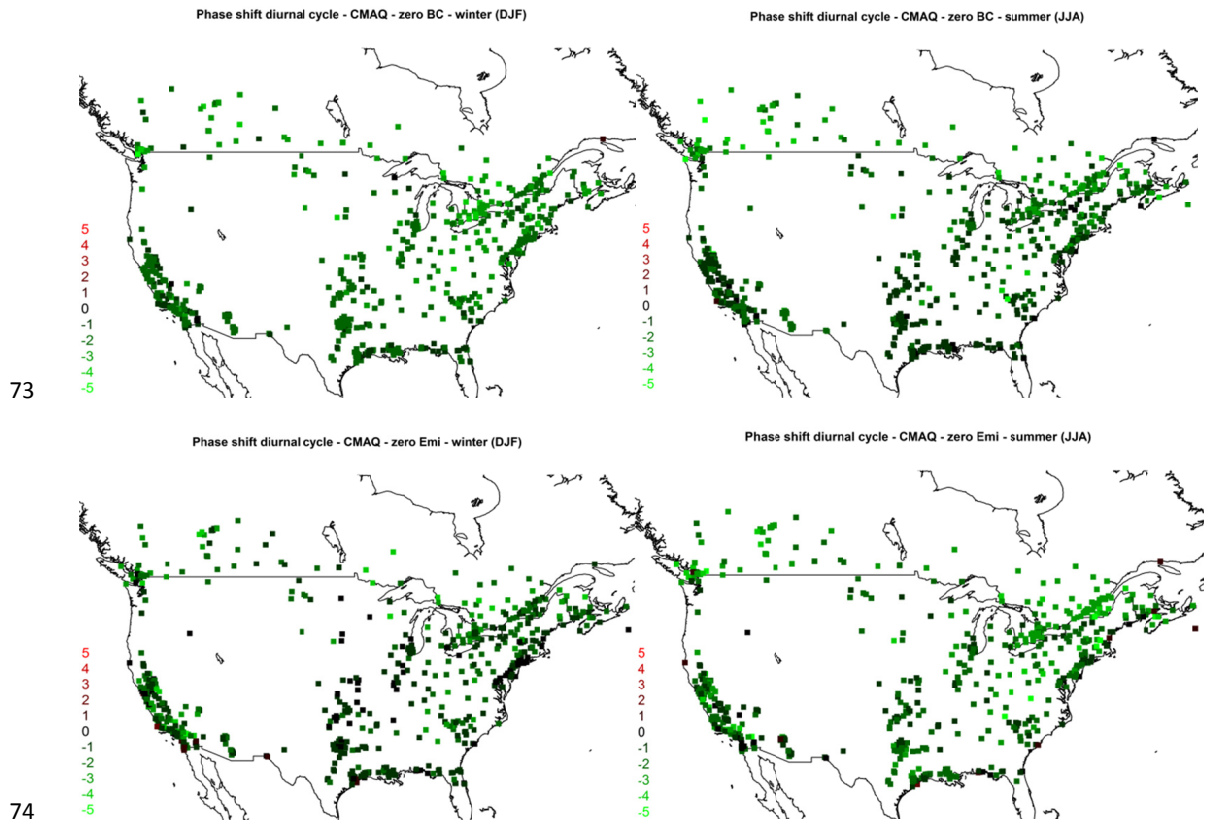


66

76 **FIGURE S12.** Autocorrelation (ACF) and partial autocorrelation (PACF) function for the differenced time series of
 77 residuals of ozone (mod-obs) for the 'zero Emi' scenario calculated at three stations where the cumulated
 78 isoprene concentration over the months of June-July-August is minimum (compatibly with the availability of
 79 and completeness of monitoring data). a) CMAQ and b) Chimere

71

72



84 **FIGURE S13.** Phase shift of the diurnal cycle (in hour) for the network of receptors in NA (includes all stations
 85 types). A positive phase shift indicates that the model peak is 'late', vice-versa if the phase shift is negative, the
 86 model peak occurs earlier than the observed peak. Top panels 'Zero BC' case (winter and summer); lower
 87 panels: 'Zero EMI' case (winter and summer)

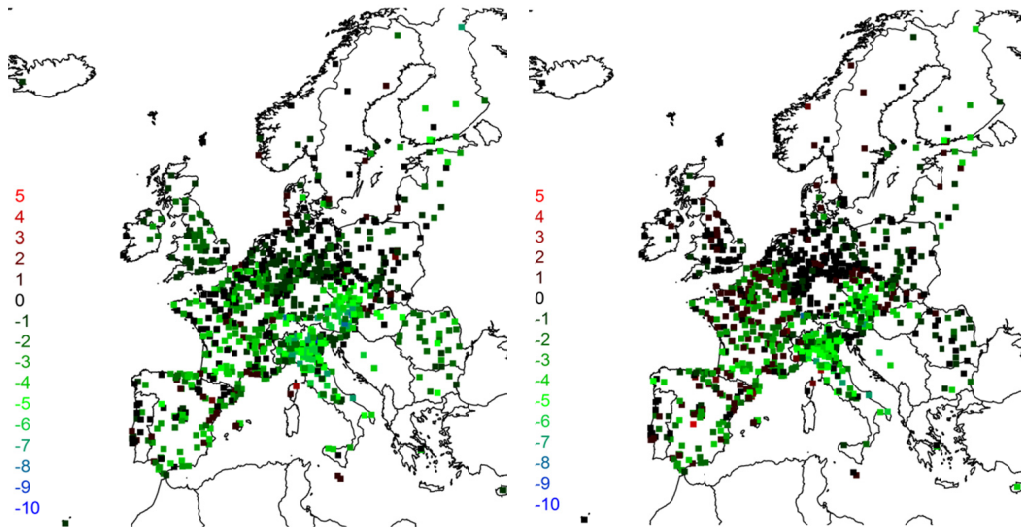
79

80

81

Phase shift diurnal cycle - Chimere - const BC - summer (JJA)

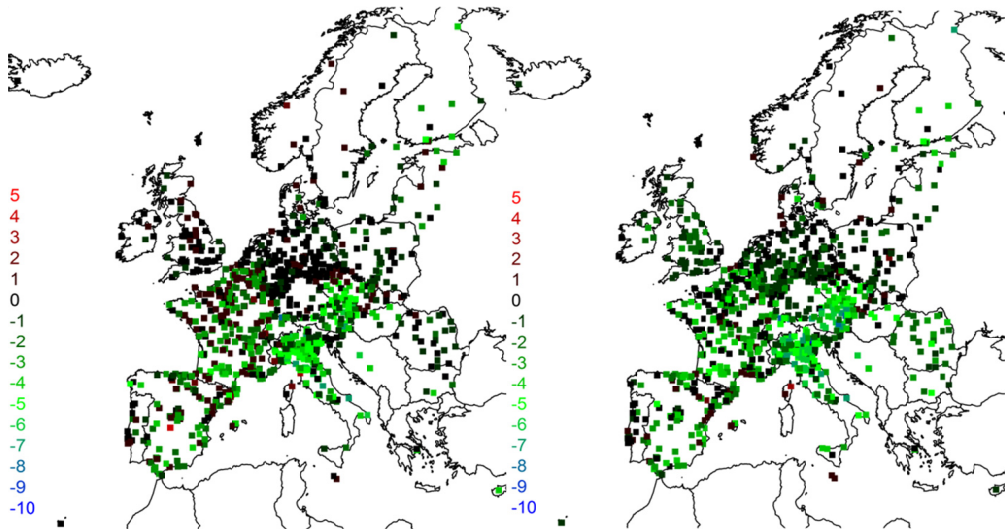
Phase shift diurnal cycle - Chimere - const BC - winter (DJF)



82

Phase shift diurnal cycle - Chimere - zero Emi - winter (DJF)

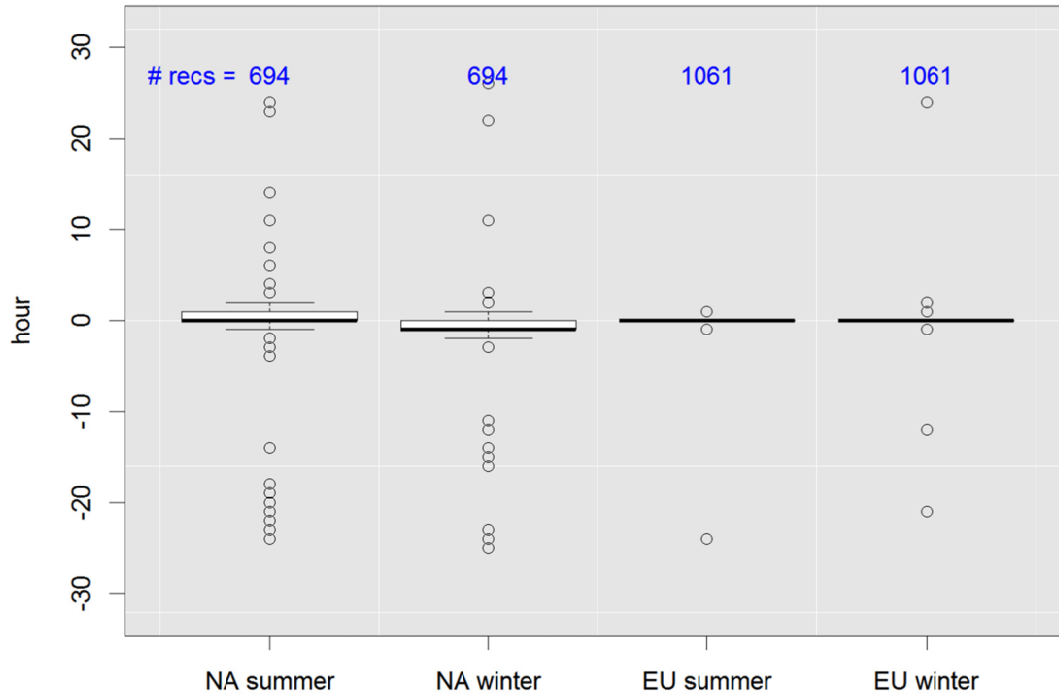
Phase shift diurnal cycle - Chimere - zero Emi - summer (JJA)



83

84 **Figure S14.** As in Figure S13 for Europe

time shift "base" - time shift "zero Emi"

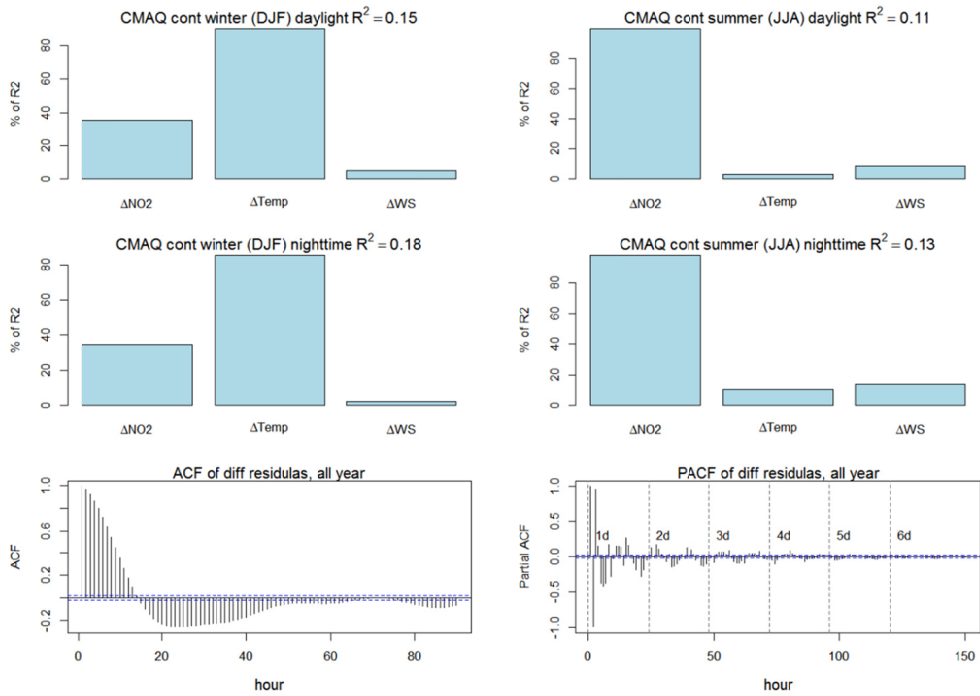


85

89 **FIGURE S15.** Percentile distribution of the difference (in hour) at the receptors (the number of receptors is
90 reported at the top) between the time shift of the base and the 'zero Emi' case

88

89

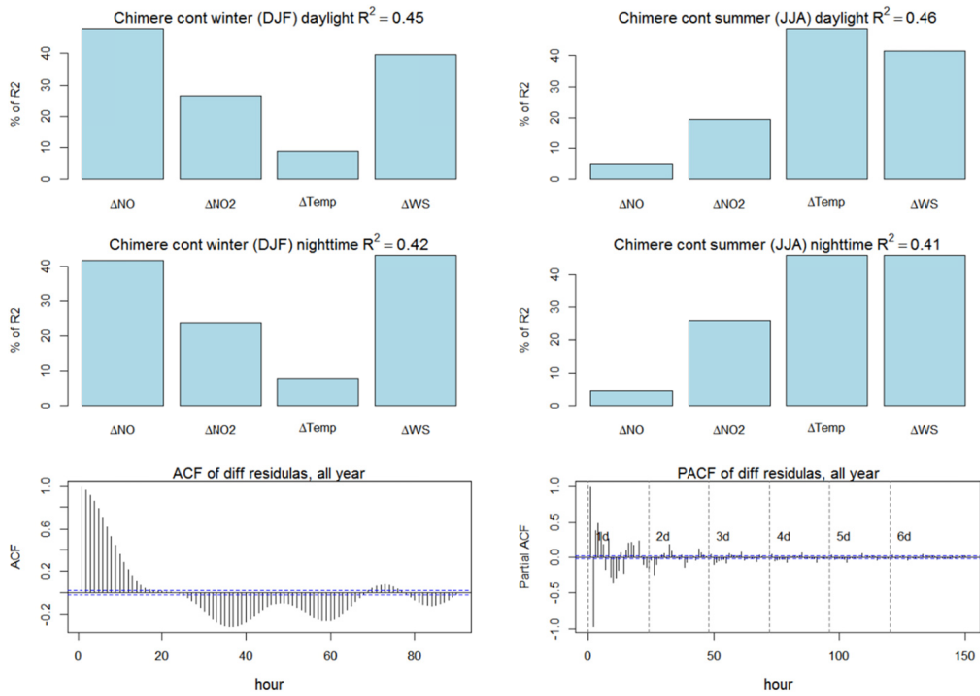


90

106 **FIGURE S16.** Percentage of variance explained by the regressors (the total R^2 for the regression is reported in the
 107 title of each panel) when the diurnal fluctuations are removed. The relative importance of each variable is
 108 assessed by using a bootstrap resampling. The plots at the bottom show the ACF and PACF of the yearly time
 109 series of residual of the fit, that is, of what is not captured by the linear regressions on the available variables. .
 110 The analysis encompasses 47 co-located stations (the NA stations for ozone, NO₂, WS, and Temp that fall in a
 111 radius of 1000 m and vertical displacement less than 250m).

97

98



99

103 **FIGURE S17.** Same as FIGURE S16 for EU. The analysis encompasses 61 co-located stations (the EU stations for
 104 ozone, NO, NO₂, WS, and Temp that fall in a radius of 1000 m and vertical displacement less than 250m).

102

103

104